Free energy calculations of small molecules in dense amorphous polymers. Effect of the initial guess configuration in molecular dynamics studies

Nico F. A. van der Vegt
Chemical Physics Laboratory and Membrane Technology Group, P.O. Box 217, 7500 AE Enschede, The Netherlands

Wim J. Briels
Chemical Physics Laboratory, P.O. Box 217, 7500 AE Enschede, The Netherlands

Matthias Wessling and Heiner Strathmann
Membrane Technology Group, P.O. Box 217, 7500 AE Enschede, The Netherlands

(Received 12 June 1996; accepted 13 August 1996)

The excess free energy of small molecules in the amorphous polymers poly(ethylene) and poly(dimethylsiloxane) was calculated, using the test-particle-insertion method. The method was applied to polymer configurations obtained from molecular dynamics simulations with differently prepared initial guess configurations. It was found that the calculated solubility coefficients strongly depend on the quality of the initial guess configuration. Slow compression of dilute systems, during which process only the repulsive parts of the nonbonded Lennard-Jones potentials are taken into account, yields polymer melts which are better relaxed, and which offer lower solubilities for guest molecules compared with polymer melts generated at the experimental density or prepared by compressing boxes with soft-core nonbonded potentials. For the last two methods initial stresses relax by straining the internal modes (bond angles, torsion angles) of the chains. © *1996 American Institute of Physics.* [S0021-9606(96)50143-1]

I. INTRODUCTION

Fundamental understanding of the permeation process of small molecules dissolved in dense polymers is important in membrane processes and the development of barrier materials. The capacity of membranes to separate gases is controlled by the affinity of the gas towards the polymer and the mobility of the gas in the polymer.

Atomistic modeling of dense amorphous polymers by means of molecular dynamics (MD) simulations has become an important tool for the study of microscopic processes.[1] Several MD studies were reported on the mechanism of gas diffusion in dense polymers.[2–4] The diffusivity of the molecule is governed by a hopping mechanism between sorption sites having a local minimum free energy. The diffusion coefficients are obtained from the mean square displacement $\langle r^2(t)\rangle$ of the dissolved molecules in the polymer matrix. In the diffusive regime the mean-square displacement should depend linearly on time, i.e., $\langle r^2(t)\rangle \propto t$, the slope being proportional to the diffusion coefficient. This approach has been applied successfully to small particles in rubbery polymers.[3]

The time scale on which the diffusive regime is reached, however, increases drastically with increasing particle size and polymer stiffness, making full atomistic MD simulation less effective. Improved simulation techniques were reported.[5,6] based on extending time scales by preaveraging the thermal vibrational modes of the polymer matrix, the diffusion process being described as an activated hopping process between low free energy sorption sites.

The affinity of the gas towards the polymer is described by the solubility or Henry constant. Calculations of the excess chemical potential of the guest particle in the polymer host matrix have been reported in the literature.[3,4,6–9] These calculations yield an overestimation of the gas solubility by one or two orders of magnitude. Table I shows some results obtained by several authors together with experimentally obtained results. It has been argued that disagreement with experiments stems from poor interaction parameters, a deviation of 2–3 kT from experimentally obtained excess free energies being rather common in free energy calculations.[10] This, however, does not explain the general phenomenon of overestimating the solubilities of small molecules in polymer matrices and it was argued that the quality of the polymer starting structure might also be responsible for the overestimation of solubilities.[7]

We will show that the detailed atomistic structure of the polymer matrix is the most important parameter that strongly influences calculated solubilities. The distribution of sorption sites should be homogeneous, i.e., an inhomogeneous matrix or the presence of a few large sorption sites in the matrix probably yields far too large solubilities. Therefore, an important effort should be made on the generation of a homogeneous microstructure containing a realistic distribution of sorption sites.

In this paper we will investigate to what extend the initial guess polymer structure influences the sorption of guest molecules in poly(ethylene) (PE) and poly(dimethylsiloxane) (PDMS) polymer membranes. Free energy calculations of molecules He, H_2, Ar, N_2, O_2, and CH_4 will be presented. Different methods for generating the microstructures were adopted. For all microstructures, solubilities were calculated. The effect of the potential energy function for the polymer was examined by comparing results for solubilities in PE, simulated with two force fields at constant *NPT* conditions. In the next sections we shall discuss the calculation of excess chemical potentials, the simulation details, the methods for

TABLE I. Solubilities[a] cm^3 (STP) cm^{-3} atm^{-1} of different small molecules obtained from MD simulations of poly(propylene) (PP), poly(dimethylsiloxane) (PDMS), poly(ethylene) (PE) and poly(isobutylene) (PIB).

	PP		PDMS		PE		PIB	
	Calc.	Expt.	Calc.	Expt.	Calc.	Expt.	Calc.	Expt.
He	0.13 (Ref. 8)	0.015 (Ref. 24)	0.17 (Ref. 4)	0.043 (Ref. 26)		0.012 (Ref. 30)	0.089 (Ref. 7)	0.011 (Ref. 25)
H_2	0.85 (Ref. 8)	0.15					1.4 (Ref. 7)	0.036 (Ref. 25)
Ar			2.0 (Ref. 4)	0.34 (Ref. 26)		0.103 (Ref. 30)		
N_2	1.6 (Ref. 8)	0.06 (Ref. 24)				0.041 (Ref. 30)		
O_2	4.4 (Ref. 8)					0.077 (Ref. 30)	10.9 (Ref. 7)	0.12 (Ref. 25)
CH_4	11.5 (Ref. 8)		10.4 (Ref. 9) 12.5 (Ref. 3)	0.45 (Ref. 27)	1.60 (Ref. 9)	0.203 (Ref. 30)		

[a]Temperatures are Ref. 8: 300 K, Ref. 24: 297.5 K, Ref. 4: 273 K, Ref. 26: 273 K, Ref. 3: 300 K, Ref. 27: 308 K, Ref. 7: 300 K, Ref. 25: 298 K, Ref. 9: 300 K, Ref. 30: 298 K for 100% amorphous polyethylene.

generating different polymer microstructures and the resulting solubilities for the above mentioned gaseous permeants in the different microstructures.

II. THE EXCESS CHEMICAL POTENTIAL

In the canonical ensemble the chemical potential $\mu(N,V,T)$ of a system containing N particles, interacting according to $\Phi(\mathbf{r}^N)$ is expressed as

$$\mu(N,V,T) = -kT \ln\left(\frac{q^{\text{int}}}{\Lambda^3}\frac{1}{N}\frac{Z_N}{Z_{N-1}}\right), \tag{1}$$

where q^{int} denotes the internal partition function of the particle. The thermal de Broglie wavelength $\Lambda=(h^2/2\pi mkT)^{1/2}$, Z_N is the configurational part of the partition function related to the interaction potential $\Phi(\mathbf{r}^N)$ by $Z_N=\int d\mathbf{r}^N \exp[-\beta\Phi(\mathbf{r}^N)]$ and $\beta=(kT)^{-1}$. For an ideal gas $Z_N/Z_{N-1}=V$; in the more general case $Z_N/Z_{N-1}=(NkT)/f$ where f is the fugacity. In actual calculations, the difficulty stems from evaluating the configurational part. Following Widom's approach,[11] we write

$$\frac{Z_N}{Z_{N-1}} = V\langle \exp(-\beta\Delta E)\rangle_{N-1} = \frac{NkT}{f}, \tag{2}$$

where ΔE is the increase in potential energy when one particle is being added to the system. This extra particle, however, should not influence the (NVT) ensemble of states from which the average is calculated.

Equation (2) can be evaluated by calculating the interaction of a gaseous particle inserted at a random place in the polymer matrix. The particle is not really inserted, however, only the ''would have been'' changes in energy are calculated. In the dilute solution limit, these changes in potential energy should arise only from the interactions of the guest molecule with the polymer atoms and not with other sorbed particles. The ''ghost'' interaction therefore reads

$$\Delta E = \sum_i^n E_i, \tag{3}$$

where i runs over all matrix atoms and E_i is the interaction between matrix atom i and the inserted particle. The interactions between a matrix atom and inserted particles are all described with Lennard-Jones potentials. We will consider here the guest particles He and Ar, and also the polyatomic molecules N_2, O_2, and CH_4. The polyatomics will be considered as spherically symmetric particles that are described with united atom potentials. We therefore assume that the internal degrees of freedom of the polyatomics are not affected by the dissolution process.

When the membrane is in equilibrium with an ideal gas of guest molecules we may replace f by P in Eq. (2), obtaining for the equilibrium concentration of the gaseous species in the polymer matrix

$$\frac{N}{V} = \beta\langle \exp(-\beta\Delta E)\rangle_{NVT} P, \tag{4}$$

where N/V denotes the number density of sorbed molecules. The average is calculated by performing random insertions in the polymer matrix, thermal averaging is achieved by subjecting the polymer matrix to MD simulation.

In many applications the number density of gas sorbed in the matrix is presented relatively to the number density of an ideal gas at standard conditions,

$$c^{\text{eq}} = V(STP)/V = SP, \tag{5}$$

where $V(STP)$ denotes the volume of ideal gas sorbed at standard temperature and pressure; $T_s=273.15$ K, $P_s=1.013$ bar, and V is the volume of the polymer sample at experimental conditions. The second equals sign in Eq. (5) serves to define the solubility constant S. Rewriting Eq. (4) yields

$$S = \frac{T_s}{P_s T}\langle \exp(-\beta\Delta E)\rangle_{NVT}. \tag{6}$$

This gives rise to units cm^3(STP) cm^{-3} bar^{-1} for S.

One advantage of the Widom approach is that for one set of polymer configurations we can calculate the excess chemical potential for several different gases. In other methods for evaluating free energy related quantities like thermodynamic integration techniques and perturbation methods[12] one has to sample configurational space separately for all species. The Widom insertion technique, on the other hand, can only be used for relative small particles, since the probability for successful insertion drastically decreases with increasing particle size. Larger permeant particles are likely to overlap with the matrix atoms resulting in large positive values for ΔE and therefore small contributions to the chemical potential.

The result will be poor statistics, that can only be improved with long simulations and by averaging the Boltzmann factor of the inserted particle over many independent polymer matrices.

The number of insertions to be performed to adequately sample the Boltzmann factor of a permeant molecule can be evaluated[13] from the product $\exp(-\beta E)\rho(E)dE$, where $\rho(E)dE$ is the probability that a permeant upon insertion experiences an energy between E and $E+dE$. To obtain reliable results, this product should be well sampled across its maximum value. Calculations reported on PDMS,[3] poly(isobutylene),[7] and poly(propylene)[8] were performed with about 10^4–10^5 insertions per polymer configuration.

Experimentally, one often obtains results at constant N, P, and T. In the NPT ensemble Eq. (6) becomes

$$S=\frac{T_s}{P_s T}\frac{\langle V\ \exp(-\beta\Delta E)\rangle_{NPT}}{\langle V\rangle_{NPT}}. \tag{7}$$

We have simulated both NPT and NVT ensembles, obtaining solubilities with Eqs. (6) and (7) which do not differ significantly.

III. SIMULATION DETAILS

MD simulations were performed on amorphous PE and PDMS systems. All PDMS boxes consisted of 12 chains of 60 monomer units $[-Si(CH_3)_2-O-]$, and the PE boxes consisted of 12 chains of 120 monomer units $[-CH_2-]$. CH_2 groups in PE and CH_3 groups in PDMS are modeled as united atoms in order to reduce the number of atoms in the actual simulation, and to be able to use larger time steps in the integration scheme. The simulated systems were all subjected to rectangular periodic boundary conditions.

Simulations were performed, using the GROMOS package.[14] Bond vibrations and bond angle vibrations were treated by a harmonic potential

$$V(b)=1/2k_b(b-b_0)^2 \tag{8}$$

for all bonds, and

$$V(\theta)=1/2k_\theta(\theta-\theta_0)^2 \tag{9}$$

for all bond angles, where b_0 and θ_0 are the equilibrium bond length and angle. The force constants for bond and bond angle vibrations are k_b and k_θ, respectively. The dihedral rotations were described with

$$V(\varphi)=k_\varphi[1+\cos(n\varphi-\delta)], \tag{10}$$

where k_φ is a force constant, n is the multiplicity factor, and δ is a phase shift. Dihedral rotations in PDMS were described with Eq. (10), dihedral rotations in PE are described with the rotational potential of Ryckaert and Bellemans,[15] i.e.,

$$V(\varphi)=\sum_{n=0}^{5} c_n\cos^n(\varphi). \tag{11}$$

The nonbonded pair interactions were represented by Lennard-Jones 12-6 potentials

$$V(r)=4\epsilon[(\sigma/r)^{12}-(\sigma/r)^6] \tag{12}$$

and electrostatic potentials

$$V(r)=\frac{q_i q_j}{4\pi\epsilon_0 r}. \tag{13}$$

Lennard-Jones and electrostatic interactions were calculated for all atom pairs, excluding bonded 1–2 and 1–3 neighbors. The 1–4 Lennard-Jones interactions were scaled[16] with a factor 0.5 in the case of PDMS, and were excluded in PE, since the Ryckaert and Bellemans rotational potential implicitly contains these interactions. A spherical cutoff $r_{LJ}=1.15$ nm was used[17] for calculating the nonbonded Lennard-Jones interactions in PE, cutoffs used for PDMS were $r_{LJ}=1.0$ nm for Lennard-Jones interactions and $r_{EL}=1.2$ nm for electrostatic interactions.[3] The force field parameters are listed in Table II.

The equations of motion were solved using the leap-frog algorithm with a time step of 2.5 fs for both PE and PDMS systems. Simulations of the NPT and NVT ensemble were performed using a weak coupling scheme to a temperature (300 K) and pressure (1 atm) bath with coupling constants of 0.1 and 0.5 ps, respectively.[18]

IV. GENERATING INITIAL STRUCTURES

Melting an idealized structure, for instance a cubic lattice structure, is a common method for preparing a starting configuration in simulations of liquids. The equilibration process involves simulating the system in the order of tens of picoseconds, which includes the important relaxation times of the system. In polymer melts, the correlation lengths and times are much longer and therefore the equilibration processes are some orders of magnitudes larger than are feasible with MD. Consequently one needs other ways of preparing initial polymer structures, that resemble the equilibrium structure as much as possible.

One method which has been used to prepare an initial polymer box, was to simply randomly generate monomer positions, and next to construct chains by introducing bonds between close neighbors.[21] A serious disadvantage of this method is the long time in which the dihedral angles relax towards their equilibrium values.

A second method concentrates on producing correct statistics for the dihedral angles in the first step of the system preparation, i.e., the generation of polymer chain conformations. One way to do this is to make use of the rotational isomeric state (RIS) model introduced by Flory.[19] Chain conformations are described by a set of discrete dihedral angles, generated according to a Boltzmann probability. Usually there are only three different states for each dihedral angle, called trans, gauche plus, and gauche minus. The potential energy is assumed to depend only on the state of the bond being assigned and on the state of the previous bond, with the all trans state as a reference. Excluded volume interactions are neglected in this model, but for polymer melts, the RIS-chain statistics describe the experimentally observed

TABLE II. Force field parameters for PDMS,[a] PE,[b] and permeant molecules.[c]

Bonds	k_b (10^5/kJ mol^{-1} nm^{-2})	b_0 (nm)
Si–O	2.5080	0.160
Si–CH_3	2.5080	0.188
CH_2–CH_2	3.3475	0.153
CH_2–CH_3	3.3475	0.153
Angles	k_Θ (kJ/mol^{-1} rad^{-2})	Θ_0 (deg)
Si–O–Si	118.4	114.0
O–Si–O	791.2	109.5
O–Si–CH_3	418.4	109.5
CH_3–Si–CH_3	418.4	109.5
CH_2–CH_2–CH_2	519.6	114.0
CH_2–CH_2–CH_3	519.6	114.0

Dihedrals	k_φ (kJ mol^{-1})	n	δ
CH_3–Si–O–Si	3.77	3	0
Si–O–Si–CH_3	3.77	3	0
Si–O–Si–O	3.77	3	0
O–Si–O–Si	3.77	3	0
CH_2–CH_2–CH_2–CH_2	5.86	3	0
CH_3–CH_2–CH_2–CH_2	5.86	3	0

Nonbonded	ϵ (kJ mol^{-1})	σ (nm)	$q(e)$	(a.m.u)
Si	2.4480	0.3385	0.3	28.080
O	0.8493	0.2955	−0.3	15.999
CH_3 (PDMS)	0.7532	0.3786	0	15.035
CH_2	0.3908	0.3930	0	14.027
CH_3 (PE)	0.9480	0.3930	0	15.035
He	0.0850	0.2580	0	4.003
H_2	0.3076	0.2950	0	2.016
Ar	0.9977	0.3400	0	39.948
N_2	0.7898	0.3700	0	28.013
O_2	0.9145	0.3500	0	31.998
CH_4	1.2466	0.3733	0	16.043

[a]Taken from Ref. 3.
[b]Taken from Ref. 17.
[c]Taken from Refs. 5 and 3 (He and CH_4).

chain properties well.[19] Because of the interactions between neighboring bonds, chains have to be generated using conditional probabilities.

Chains generated according to this formalizm have been used as starting configurations in MD simulation, by placing them at random positions in the simulation box at the experimental density.[20] This method has the severe disadvantage of introducing a significant amount of overlaps, and therefore, enormous potential energies at the start of the simulation. Furthermore the risk of obtaining structures with large density fluctuations and even with unrealistically large regions of empty space, is very high. It has been attempted to remedy these problems by growing the chains by means of Monte Carlo methods directly into the box. Theodorou and Suter[23] used the RIS model to generate trial configurations with the correct statistics of fixed dihedral angles, and included excluded volume effects in the Monte Carlo step. Clarke and Brown[22] used a similar methodology by using continuous dihedral angles; the trial step was done by drawing from a distribution based on the single bond contribution to the energy. These methods yield relatively homogeneous boxes compared to the method in which long range excluded volume effects are neglected. High potential energies arising from severe overlaps are avoided. It was found,[7] however, that permeant solubilities are largely overestimated with these boxes, indicating that they probably still are much too inhomogeneous.

Yet another method to accelerate the equilibration processes has been reported,[3] based on the use of soft-core nonbonded interactions. A dilute box of several chains subject to the usual periodic boundary condition was compressed, while using soft-core potentials replacing the nonbonded repulsive potentials. The full bonded interaction terms were maintained. If the shrinking is done slowly, the chains get the opportunity to relax while still in a dilute environment. Once the box has shrunk to its intended volume, the full potential is turned on and the production run is started.

A disadvantage of growing chains into a box is that the heads of the chains will eventually get trapped in regions of high density. We think that the best candidate for preparing realistic boxes is the method of shrinking boxes. However a diminished repulsion, may produce configurations which develop a lot of strain in the dihedral angles when finally the full repulsion is turned on. We suggest to remedy this by

retaining the full repulsive part of the potential during the shrinking period. Similarly, retaining the attractive part of the potential during the shrinking part of the run, may lead to clustering of the system, which will remain at all later times. Therefore, just like Sok and Berendsen, we turn off the attractive part of the potential during the shrinking stage of the run.

We start the shrinking with a configuration obtained by randomly distributed RIS chains in the box, expecting that this ensures perfect entanglement of the chains at the end of the box preparation.

We will show the important effect of the initial structures on the solubility constants of guest molecules by comparing differently prepared polymer structures. We expect improved solubility constants for boxes that are better relaxed. Different boxes were prepared by different methodologies as described below. All structures were generated using chain conformations obtained with the RIS formalism. The RIS statistical weight matrices were calculated using the parameters from the MD force field, according to the methods developed by Flory.[19] For PE we used the rotational potential of Ryckaert and Bellemans[15] that implicitly contains the 1–4 interactions. The calculated statistical weight matrix for PE shows only small deviations from the one reported by Flory.[19] We calculated the PDMS statistical weight matrix with a scaling factor 0.5 for 1–4 nonbonded Lennard-Jones interactions in PDMS.

The details of the generation of the different boxes are as follows:

(i) The first method involves generating different RIS chains that were randomly placed in the cubic simulation cell at the experimental density. This structure was energy minimized, using a steepest descend routine, to remove severe overlaps between monomer units. The system was equilibrated at *NPT* conditions during 1000 ps at 300 K and 1 atm. Calculations were performed using the trajectory of a 500 ps *NPT* production run. This method was applied to both PE and PDMS.

(ii) In the second method, RIS chains were placed in a box that has a volume of approximately eight times the experimental volume. The box was first energy minimized with the full Lennard-Jones and electrostatic potential. Then the box was shrunk according to the method described by Sok and Berendsen.[3] The full bonded potential was applied, nonbonded Lennard-Jones interactions were replaced by a soft-core potential and electrostatic interactions were neglected. The shrinking procedure was performed very slowly by gradually increasing the pressure of the external bath; the real density is reached after a time span of 750 ps. At the experimental density, the system was energy minimized with the full Lennard-Jones and electrostatic interaction and equilibrated at *NPT* conditions during 1000 ps at 300 K and 1 atm. Calculations were performed using the trajectory of a 500 ps *NPT* production run. This method was applied for PDMS and PE.

(iii) The third method resembles the second method, however, here we used the repulsive part of the Lennard-Jones interactions instead of soft-core interactions. The attractive tail of the Lennard Jones potential is left out to avoid monomers to stick together when the box is still very dilute. We started with an energy minimization with the repulsive potential, then the shrinking procedure was performed during a time span of about 500 ps. In both the energy minimization and shrinking procedure the electrostatic interactions were neglected. After the experimental density has been reached, the full Lennard-Jones and electrostatic interaction was gradually introduced in three steps of 5 ps each and the system is equilibrated at *NPT* conditions during 1000 ps at 300 K and 1 atm. This method was applied for both PE and PDMS. Production runs were performed during 500 ps at *NPT* conditions for PDMS and PE.

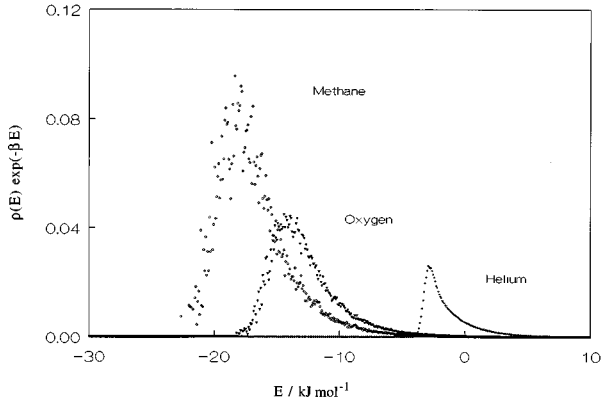

FIG. 1. $\rho(E)\exp(-\beta E)$ for helium, oxygen, and methane in PE obtained from 3×10^7 insertions during 500 ps *NPT* simulation.

V. RESULTS AND DISCUSSION

Solubilities were calculated for all generated PE and PDMS polymer structures. To sample the phase space of the inserted particle entirely, we found 60 000 insertions in every PE sample to be sufficient. In PDMS 125 000 insertions were performed. The number of insertions approximately scales with the volume of the polymer box. Averages were calculated from 500 coordinate sets taken every picosecond from a 500 ps simulation. Figure 1 shows the product $\exp(-\beta E)\rho(E)$ for a PE structure for several permeants. Increasing the number of insertions did not improve the poor sampling of low energy regions for CH_4. As a consequence rather high standard deviations are found for the solubility of the larger particles. The reason for this bad statistics can be understood by noticing that the tails of $\rho(E)$ are necessarily badly sampled. Since the Boltzmann factor very much favors the low energy tail, the sampling of this tail dictates the overall statistics. Since $\rho(E)$ shifts to the right with increasing permeant size, this effect is more important for large permeants. Longer simulations therefore are necessary to obtain solubilities for molecules that have about the size of methane. One should average over different polymer structures to improve predictions, this will, however, cost a huge amount of computational power.

The convergence of the excess free energies was studied by extending the molecular dynamics simulation for a PE

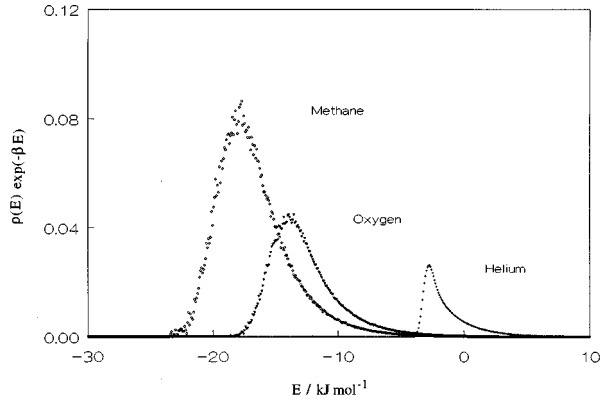

FIG. 2. $\rho(E)\exp(-\beta E)$ for helium, oxygen, and methane in PE obtained from 3×10^8 insertions during 5 ns *NPT* simulation.

sample generated by the slow compression method. Excess free energies were calculated from a 5 ns run, in which coordinates were stored every 1 ps. A total number of 3×10^8 test-particle insertions were performed in 5000 coordinates sets for each of He, H_2, N_2, O_2, Ar, and CH_4. From Fig. 2 it is seen that $\exp(-\beta E)\rho(E)$ is well sampled now, also for the larger permeants. It is clear that a well converged excess free energy can be obtained for He from a 500 ps run, but that for the larger permeants such as methane, the excess free energy converges only after several nanoseconds. This we see even more clearly from Fig. 3. Here solubility constants for H_2, N_2, Ar, and CH_4 are displayed which are averaged over consecutive time intervals of 500 ps out of a run of 5 ns. The smaller permeants clearly show smaller scatter than the larger ones, even on a normalized scale. It is also seen that runtimes, long enough to obtain good statistics, vary from 500 ps for Helium to several nanoseconds for methane. We should notice however that the statistical error of the solubility constants can only be obtained by using several independent similarly prepared boxes (*vide infra*).

Solubilities were calculated for both the PDMS and PE microstructures using the same cutoff for nonbonded interactions between inserted particle and the matrix atoms. The cutoff distance $R_c=11.5$ Å was used. At this distance, the Lennard-Jones interactions between the permeant and a polymer atom have decreased to about -0.005ϵ in the worst case. In principle a long range correction should be applied on the insertion energy;[8]

$$\Delta E_{\text{insert}}^{\text{long range}}=\sum_{\alpha}\int_{R_c}^{\infty} dr\ 4\pi r^2\rho_\alpha g_\alpha(r)\varphi_\alpha(r), \tag{14}$$

where α numbers different matrix atom types, ρ_α is the number density of atom type α, and $\varphi_\alpha(r)$ the interaction potential for the inserted particle and atom type α pairs. The inserted particle is assumed to experience a mean field beyond the cutoff distance R_c, i.e., the radial distribution function $g_\alpha(r)$ for inserted particle and matrix atoms α beyond R_c equals one. Table III shows the effect of a long range correction on the solubility of gases in PDMS calculated with a PDMS polymer sample generated by random positioning of the centers of mass of 12 PDMS RIS chains in the simulation box at experimental density. Clearly the long range effect becomes more important for larger permeant particles with a higher Lennard-Jones well depth. The long range correction was used in all calculations of the solubility of the different gases in both PDMS and PE.

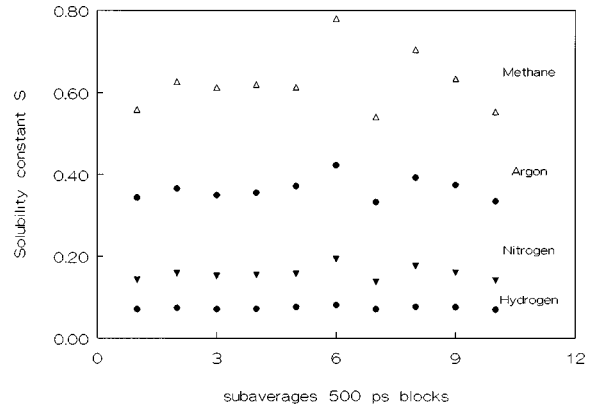

FIG. 3. Solubility constants $\text{cm}^3\,\text{STP}\,\text{cm}^{-3}\,\text{bar}^{-1}$ in increasing order for hydrogen, nitrogen, argon, and methane in PE. Shown are the averages over 500 ps blocks, from a total run of 5 ns.

TABLE III. Solubilities[a] of permeants in PDMS calculated with the mean-field approximation beyond the spherical cutoff distance.

Permeant	Cutoff	Mean-field correction
He	0.13	0.13
H_2	0.23	0.25
Ar	1.76	2.29
N_2	1.16	1.57
O_2	1.49	1.96
CH_4	4.73	7.00

[a]Units cm^3 (STP) $\text{cm}^{-3}\,\text{bar}^{-1}$.

A. PDMS

Solubilities of different guest molecules in differently prepared PDMS boxes are shown in Table IV. As expected, by randomly placing the chains at the experimental density, we overestimate the solubility constant with a factor 2–14. This overestimation is found for two samples, i.e., two statistically independent boxes prepared with the same method. The boxes prepared by slow compressing dilute systems show improved solubility constants. Compressing the box with repulsive nonbonded potentials yields solubility constants in rather good agreement with the experimental values when compressed slow enough. The solubilities of He and H_2 are in good agreement with the experimental values, deviation increases as the permeants size increases. One may speculate that larger permeants are a more sensitive probe to structural inhomogeneous places in the polymer matrix. Compressing the box using soft-core nonbonded potentials yields worse solubility constants compared to the compression with repulsive nonbonded potentials despite the slow compression time of 600 ps.

TABLE IV. Solubilities[a] of permeant molecules in different PDMS matrices at 300 K.

Method	Random positioning at experimental density		Softcore slow compression[b]	Compressing at different velocities[c] with repulsive potentials			Experiment
Permeant	Sample 1 $\langle V_{box}\rangle$=84.89[d]	Sample 2 $\langle V_{box}\rangle$=83.99	Sample 1 $\langle V_{box}\rangle$=83.16	Sample 1 $\langle V_{box}\rangle$=81.54	Sample 2 $\langle V_{box}\rangle$=80.03	Sample 3 $\langle V_{box}\rangle$=80.43	298 K
He	0.13	0.12	0.091	0.082	0.058	0.063	0.043[e](273K)
H_2	0.25	0.24	0.18	0.16	0.098	0.109	0.074[e](273K)
Ar	2.29	2.36	2.05	1.91	1.05	1.18	0.256[f]
N_2	1.57	1.58	1.24	1.08	0.46	0.48	0.127[f]
O_2	1.96	2.01	1.68	1.53	0.78	0.84	0.224[f]
CH_4	7.00	7.21	6.81	6.78	2.73	2.92	0.53[f]

[a]Units cm^3 (STP) cm^{-3} bar^{-1}.
[b]Box compressed in 600 ps.
[c]Sample 1: box generated in 60 ps, sample 2: box generated in 275 ps, sample 3: box generated in 550 ps.
[d]Average box volumes in units nm^3.
[e]Reference 26.
[f]Reference 28.

The solubility constants are extremely sensitive to the density of the simulated system. The average box volume calculated from production runs decreases by almost 5 nm^3 (about 6%) when the box is slowly compressed with repulsive nonbonded potentials. These boxes have a higher density and hence less free space and lower solubility constants. It is thus possible to generate boxes with a different density when different generation methods are applied. One therefore cannot distinguish *NPT* and *NVT* simulations since during *NPT* runs the density will not adjust whereas during *NVT* runs the equilibrium pressure will not be reached both due to the slow relaxation processes. A *NPT* run can therefore be considered as a *NVT* at the volume determined with the generation method. Notice that the density reached with the compressing methods does not depend on how far we compress the box. This was examined by compressing two identical boxes. The first box was compressed too far (ρ $=1.43$ g cm^{-3}) and consequently relaxed during equilibration by expanding. The other box was compressed less far ($\rho=0.83$ g cm^{-3}) and relaxed during equilibration by shrinking towards the final density of the first box.

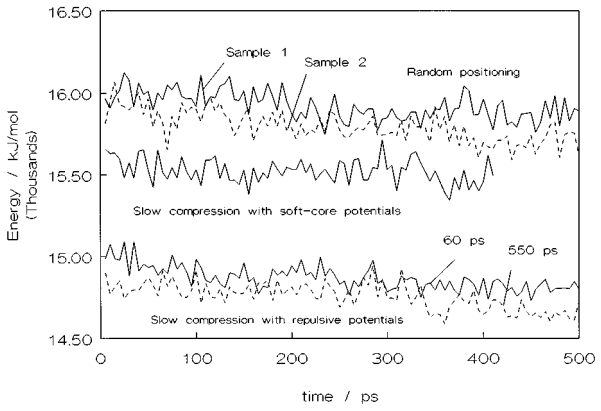

FIG. 4. Total energy of different PDMS structures during a 500 ps *NPT* molecular dynamics run at 300 K and 1 atm.

The boxes generated by random positioning of chains at the experimental density or by slow compression with softcore nonbonded potentials get trapped at the generated systems volume. The chains relax by straining angles and dihedral angles locally once the full potential is introduced. This can be explained from Fig. 4. Here the total energy of the differently prepared boxes is plotted against the simulation time during the production runs. Clearly the boxes prepared by randomly placing the chains at the experimental density show the highest energy. Boxes prepared by slow compression with repulsive non bonded potentials show the lowest energy. The difference between the lowest and the highest energy box corresponds to 0.16 kT per atom of the box. The energy difference between the boxes was examined with respect to the contributions arising from intra- and interchain contributions. We indeed found that these differences up to 70% arise from single (intra) chain contributions. The contributions mainly arise from angles, dihedral angles and 1–4 and 1–5 nonbonded interactions along the chains. These chains thus are highly strained compared to the chains in the lowest energy box.

The size distribution of sorption sites will depend on the systems density and should be broader for less dense systems. The solubility of different permeants will be higher for boxes with a broader distribution. The size distribution of sorption sites was examined by considering the insertion probabilities of hard spheres for the differently prepared boxes. The insertion probability $P(R)$ is defined as the probability that a hard sphere solute of radius R can be inserted at an arbitrary point in the polymer matrix without overlap with the van der Waals volume of any matrix atom. Each matrix atom is then considered as a hard sphere with radius $\sigma/2$, where σ is the Lennard-Jones size parameter. $P(R)$ is calculated as

$$P(R)=\int_R^\infty dR' P_m(R'). \tag{15}$$

This function defines $P_m(R)$, the probability that a sphere with radius within dR of R exactly fits at an arbitrary point

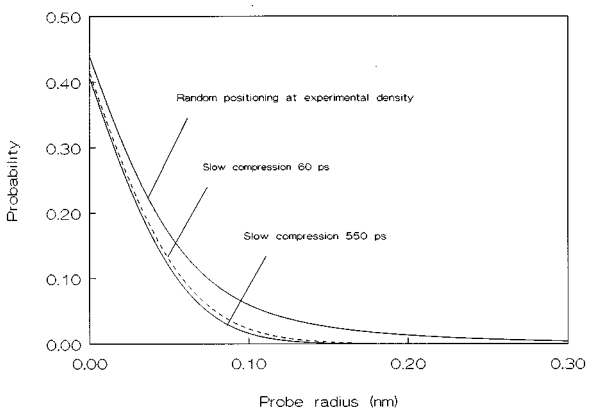

FIG. 5. Insertion probability of hard-sphere probe particles in different PDMS structures. Effect of polymer sample preparation.

in the matrix. This function is calculated by defining a $100 \times 100 \times 100$ grid inside the matrix. From every grid position the minimum distance R to the surface of a hard sphere is calculated leading to the histogram $P_m(R)$. Thermal averaging of $P_m(R)$ results in combination with Eq. (16) the insertion probability $P(R)$. For hard-sphere interactions, $P(R)$ is directly related to the solubility of the guest particle. The insertion probability is qualitatively related to the free volume and its distribution and therefore gives an indication of the distribution of low free energy sorption sites. Moreover it should provide information to what extend the simulated structures have relaxed towards a denser system. Figure 5 shows the insertion probabilities for different PDMS boxes. Clearly the box in which the chains were placed at random at the experimental density, shows a broad probability distribution. The boxes that were slowly shrunk were able to relax and show a much more narrow distribution. A broad distribution indicates the existence of larger low energy sorption sites which lead to an overestimation of the solubility coefficients of small permeants, since the test-particle insertions in these regions yield large contributions to the excess chemical potential.

B. PE

Polyethylene boxes were prepared following the same methodology as for PDMS. The forcefield used for PE predicted good phase behavior for *n*-alkane systems.[17] A second united atom forcefield was taken from GROMOS to study the effect of choosing different potentials for the same PE system on the gas solubilities. In all simulations, initial structures consisted of 12 RIS chains. Table V lists the solubilities of different permeants in the different PE structures. Here the effect of the preparation method on the solubilities is smaller compared to the PDMS boxes but still present. Random positioning RIS chains at the experimental density and slowly compressing dilute boxes with the soft-core nonbonded potential yield boxes with higher permeant solubilities compared to the boxes compressed with the repulsive part of the nonbonded potential. Compressing boxes was in all cases performed within 700 ps starting with an eight times too low density. Three statistically independent boxes were prepared with repulsive nonbonded potentials during the shrinking procedure. For these three boxes solubilities are lower compared to the other two preparation methods. We therefore may safely conclude that the same trend is observed as for the PDMS boxes. From the total energy of PE boxes we find a smaller differences compared to the PDMS boxes. The box prepared by slow shrinking with soft-core potentials has an average energy of 0.1 kT per atom more compared to the box compressed with the repulsive part of the nonbonded potential. Again this difference arises to the largest extend from the straining of angles and dihedral angles. The average densities of the PE structures compressed with repulsive nonbonded potentials, $\rho = 0.848$ g cm^{-3}, are the closest to the experimental value $\rho = 0.85$ g cm^{-3}. Slow compressing the box with soft-core potentials yields $\rho = 0.836$ g cm^{-3}. Still the systems have a density that is slightly too low. Differences in the size distribution of the sorption sites could not be observed for the different boxes due to the small density differences.

Solubilities were calculated from a simulation with the GROMOS united atom potential for PE. In this simulation the system size was exactly the same as in the other PE simula-

TABLE V. Solubilities[a] of permeant molecules in different PE matrices at 300 K.

Method	Random positioning at exp. density	Softcore slow compression	Slow compression with repulsive potentials			Experiment[b]
Permeant	Sample 1 $\langle V_{box}\rangle = 40.01$[c]	Sample 1 $\langle V_{box}\rangle = 40.19$	Sample 1 $\langle V_{box}\rangle = 39.61$	Sample 2 $\langle V_{box}\rangle = 39.64$	Sample 3 $\langle V_{box}\rangle = 39.60$	
He	0.066	0.070	0.053	0.060	0.058	0.012
H_2	0.09	0.10	0.07	0.08	0.08	
Ar	0.42	0.51	0.31	0.38	0.34	0.103
N_2	0.18	0.22	0.13	0.16	0.13	0.041
O_2	0.32	0.38	0.23	0.28	0.24	0.077
CH_4	0.71	0.91	0.53	0.65	0.54	0.203

[a]Units cm^3 (STP) cm^{-3} bar^{-1}.
[b]Reference 30 for 100% amorphous polyethylene.
[c]Average box volumes in units nm^3.

TABLE VI. Solubilities of permeant molecules in PE, simulated with the GROMOS potential. The average box volume from a 500 ps production run $\langle V_{box}\rangle = 36.86$ nm^3.

Permeant	Solubility[a]	Experiment
He	0.021	0.012
H_2	0.024	
Ar	0.16	0.103
N_2	0.047	0.041
O_2	0.11	0.077
CH_4	0.27	0.203

[a]cm^{-3} (STP) cm^{-3} bar^{-1}.

tions; 12 RIS chains with the same length were placed at a random position inside the simulation box at experimental density. This system was then energy minimized using a steepest descent routine and equilibrated during 1 ns at constant NPT (1 atm and 300 K). The calculations were performed on the coordinates obtained from a 500 ps production run. The average density from this simulation $\rho = 0.91$ g cm^{-3} was higher than the ones performed with the potential taken from Smit *et al.*[17] Resulting solubilities are listed in Table VI and show better agreement with experiment which is what one expects on the basis of the higher density. The overestimation of the solubilities, while simulating too high a density, can be caused by several factors. First the preparation method has an effect as we see from Table V. Secondly the combination rules describing the interaction between unlike molecules are known to overestimate the interaction strength.[29] As a last point we mention that the choice of a different force field for the permeant molecules can result in a factor of two for the resulting solubilities, as was shown by Müller-Plathe.[7] A higher Lennard-Jones energy parameter will result in a higher solubility.

VI. SUMMARY

Due to large correlation lengths and times, nonequilibrium states of polymer melts cannot be equilibrated with MD simulation methods on present day computers. Creating well relaxed initial boxes for MD simulations, therefore, is an important step in the simulation of chain molecules. Solubilities of small gaseous molecules in amorphous structures are very sensitive to the density and homogeneity of the amorphous matrix, and are therefore perfectly suited to probe the extend of relaxation of the amorphous melts. PDMS and PE were studied as model systems. Dense polymer matrices were obtained by slowly shrinking a dilute box using only the repulsive part of the Lennard-Jones potential to describe nonbonded interactions. Boxes prepared by randomly placing RIS chains at the experimental density or by slowly compressing dilute boxes using soft-core nonbonded potentials contain chains which can only relax initial atomic overlaps by straining bond angles and dihedral angles. These latter stresses do not relax during any reasonable simulation time. Solubility constants of small permeants in these boxes are significantly in disagreement with experimental results; those obtained from boxes prepared by compressing with repulsive potentials agree much better with experiments.

Although solubilities obtained with several permeants in PE and PDMS still are somewhat high compared with experiment, they very well reproduce trends in series of increasing solubility. This will be very helpful for predicting the selective properties of a polymer for different gaseous species.

[1] F. Müller-Plathe, Acta Polym. **45**, 259 (1994).
[2] H. Takeuchi, J. Chem. Phys. **93**, 2062 (1990).
[3] R. M. Sok and H. J. C. Berendsen, J. Chem. Phys. **96**, 4699 (1992).
[4] A. A. Gusev, F. Müller-Plathe, W. F. van Gunsteren, and U. W. Suter, Adv. Pol. Sci. **116**, 207 (1994).
[5] A. A. Gusev, S. Arizzi, and U. W. Suter, J. Chem. Phys. **99**, 2221 (1993).
[6] A. A. Gusev and U. W. Suter, J. Chem. Phys. **99**, 2228 (1993).
[7] F. Müller-Plathe, S. C. Rogers, and W. F. van Gunsteren, J. Chem. Phys. **98**, 9895 (1993).
[8] F. Müller-Plathe, Macromolecules **24**, 6475 (1991).
[9] Y. Tamai, H. Tanaka, and K. Nakanishi, Macromolecules **28**, 2544 (1995).
[10] W. F. van Gunsteren and H. J. C. Berendsen, Angew. Chem. Int. Ed. Engl. **29**, 992 (1990).
[11] B. Widom, J. Chem. Phys. **39**, 2802 (1963).
[12] T. P. Straatsma and J. A. McCammon, J. Chem. Phys. **95**, 1175 (1991).
[13] M. P. Allen and D. J. Tildesley, *Computer Simulation of Liquids* (Clarendon, Oxford, 1987).
[14] H. J. C. Berendsen and W. F. van Gunsteren, *GROMOS Reference Manual* (University of Groningen, Groningen, 1987).
[15] J.-P. Ryckaert and A. Bellemans, Mol. Phys. **44**, 68 (1981).
[16] M. Billeter, A. E. Howard, I. D. Kuntz, and P. A. Kollman, J. Am. Chem. Soc. **110**, 8385 (1988).
[17] B. Smit, S. Karaborni, and J. I. Siepmann, J. Chem. Phys. **102**, 2126 (1995).
[18] H. J. C. Berendsen, J. P. M. Postma, W. F. van Gunsteren, and A. Di Nola, J. Chem. Phys. **81**, 3684 (1984).
[19] P. J. Flory, *Statistical Mechanics of Chain Molecules* (Wiley, New York, 1969).
[20] F. Müller-Plathe, J. Chem. Phys. **94**, 3192 (1991).
[21] D. Rigby and Ryong-Joon Roe, J. Chem. Phys. **87**, 7285 (1987).
[22] J. H. R. Clarke and D. Brown, Mol. Sim. **3**, 27 (1989).
[23] D. N. Theodorou and U. W. Suter, Macromolecules **18**, 1467 (1985).
[24] D. R. Paul, A. T. DiBenedetto, J. Pol. Sci. Part. C: Pol. Symp. **10**, 17 (1965).
[25] G. J. van Amerongen, J. Pol. Sci. **5**, 307 (1950).
[26] R. M. Barrer and H. T. Chio, J. Pol. Sci. C **10**, 111 (1965).
[27] V. M. Shah, B. J. Hardy, and S. A. Stern, J. Pol. Sci. B **24**, 2033 (1986).
[28] Y. Kamiya, Y. Naito, and T. Hirose, J. Pol. Sci. B **28**, 1297 (1990).
[29] G. C. Maitland, M. Rigby, E. B. Smith, and W. A. Wakeham, *Intermolecular Forces* (Clarendon, Oxford, 1981).
[30] A. S. Michaels and H. J. Bixler, J. Pol. Sci. B **50**, 393 (1961).